Journal of Molecular Graphics and Modelling 38 (2012) 298–303

Contents lists available at SciVerse ScienceDirect

Journal of Molecular Graphics and Modelling

journal homepage: www.elsevier.com/locate/JMGM

Comparative study on activation mechanism of carboxypeptidase A1, A2 and B: First insights from steered molecular dynamics simulations

Jitrayut Jitonnom[a,*], Christoph Sontag[a,b]

[a] Department of Chemistry, School of Science, University of Phayao, Phayao 56000, Thailand
[b] Demonstration School University of Phayao, Phayao 56000, Thailand

ARTICLE INFO

Article history:
Accepted 11 September 2012
Available online 23 September 2012

Keywords:
Zymogen activation
Procarboxypeptidases
Steered molecular dynamics simulation
Proteolytic cleavage

ABSTRACT

Different forms of procarboxypeptidases (PCPs) zymogens are observed experimentally to show different rates and modes of activation: PCPA1 shows a slow, biphasic, activation pathway compared to PCPA2 and PCPB which have a faster, monotonic activation behavior. Detailed mechanisms involved in activating these zymogen forms to the active enzymes are not well understood yet. In this work, three PCP zymogens (subtypes A1, A2 and B) were in silico converted into the primary cleavage state of zymogens using available X-ray structures. Based on these cleaved forms of zymogen, we are able to investigate their spontaneous dissociation process of the prosegment from its associated enzyme domain using steered molecular dynamics simulation. The simulations revealed the highest rupture force in PCPB followed by PCPA2 and PCPA1. We also found that the cleavage substantially destabilizes most of the hydrogen bonds at the prosegment–enzyme interface in each zymogen structure. The mechanisms of the prosegment unbinding seem to be similar in both PCPA1 and PCPB but different in PCPA2: PCPA1 and PCPB show first rupture in the connecting segment followed by the globular domain, while PCPA2 conversely shows first rupture in the globular domain and then in the connecting segment. Our simulations have included the dynamic and long range conformational effects taking place after the first proteolytic cleavage in PCPs, providing first insights into the activation of carboxypeptidase A1, A2 and B.

1. Introduction

Pancreatic and pancreatic-like carboxypeptidases (CPs) are a family of zinc-containing exopeptidases, involved in the digestion process, which catalyze hydrolysis of C-terminal amino acids from their substrates [1–3]. They are naturally secreted as inactive precursors or zymogens (known as procarboxypeptidases, PCPs) and are subsequently activated by proteolytic cleavage of trypsin-like protease, resulting in the release of prosegment and full activation [4].

The inhibitory role of the prosegment is essential for many biological processes as it is the nature's way of preventing undesired activation and proteolysis [5]. Some features of this prosegment in PCPs have been emerged and were discussed twenty years ago [6]. Since then, little information about the prosegment inhibition and activation has been gained, particularly only limited details of activation mechanisms of metallo-carboxypeptidase zymogens. Among these zymogens, PCPA1, PCPA2 and PCPB were intensively described and different rate and mode of activation between these three PCPs were found experimentally [7–9]. Although both PCPA1 and PCPA2 show sequences and structures similarity (Fig. 1), PCPA2 shows a much more similar inhibition mode to PCPB than to PCPA1. Furthermore, PCPA1 shows a slow activation rate compared to both PCPA2 and PCPB. Analysis of the structure alone does not fit with this result, as had been evident by several studies [6,10–14]. It is believed that these differences could be primarily due to a slower degradation of the prosegment in PCPA1 as well as to a remaining inhibitory capability of large fragments of the segment after cleavage [10].

The cleavage sites of PCPA1, PCPA2 and PCPB were identified and an elaborate activation process involving the breakdown of the scissile peptide bonds assisted by some proteases (usually trypsin) is proposed. In both porcine PCPA1 and PCPB, the first tryptic cleavage occurs at an arginyl peptide bond located in the pro-mature junction (see Fig. 1). The first cleavage in PCPA1 is followed by a trimming of the C-terminus of the prosegment by the generated CPA1 and by a second tryptic cleavage at the peptide bond Arg74p–Tyr75p, far upstream within strand 4 at the globular domain of the prosegment. Both types of cleavage are required for full activation [7]. The first cleavage in PCPB is followed by a trimming of the C-terminal residue of the prosegment by the generated CPB, and by a second tryptic cleavage at the Arg83p–Ser84p peptide bond in the N-terminal part of helix 3. However, in this case, the first tryptic cleavage is sufficient to generate full activity [8,14].

* Corresponding author. Tel.: +66 0 5446 6666x1834; fax: +66 0 5446 6664.
E-mail address: jitrayut.018@gmail.com (J. Jitonnom).

1093-3263/$ – see front matter © 2012 Elsevier Inc. All rights reserved.
http://dx.doi.org/10.1016/j.jmgm.2012.09.002

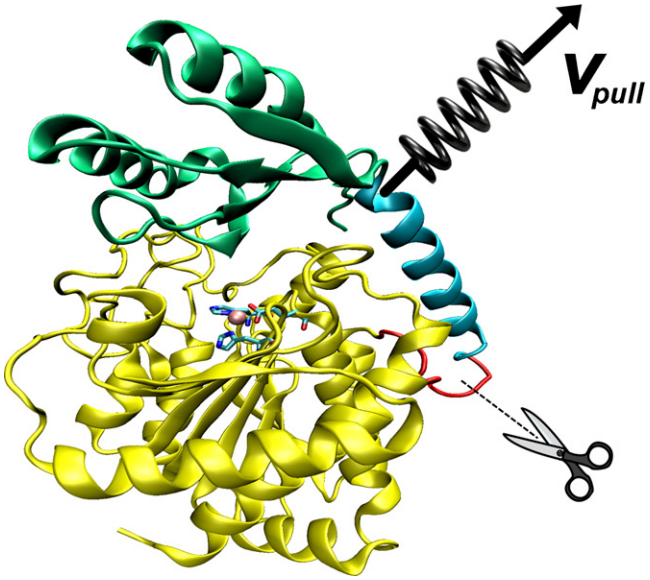

Fig. 1. Ribbon schematic representations of procarboxypeptidase whose structure is indicated in color: globular region and connecting segment of prosegment are shown in green and blue, respectively, and catalytic domain is shown in yellow. The pro-mature junction is also indicated in red. The first trypic cleavage site and the direction of the pulling potential for SMD are also indicated. (For interpretation of the references to color in this figure legend, the reader is referred to the web version of the article.)

Steered molecular dynamics (SMD) simulations, as inspired by the atomic force microscopy technique, have been used extensively to study the binding and unbinding properties of biomolecules and their responses to external mechanical manipulations at the atomic level [15,16]. Its application on the study of zymogen activation can be found from the work of Zuo and co-workers [17], as example. They have reported the activation mechanism of β-secretase zymogen using the SMD simulations and explained why β-secretase zymogen exhibits catalytic activity.

We have recently studied the dynamic behaviors of PCPA1, PCPA2 and PCPB by using MD simulation and showed flexibility among these enzymes and particularly the difference of conformational change between PCPA and PCPB [18]. Here, we further investigate at atomic level the dissociation/unbinding process of the prosegment from its catalytically binding domain with the hope

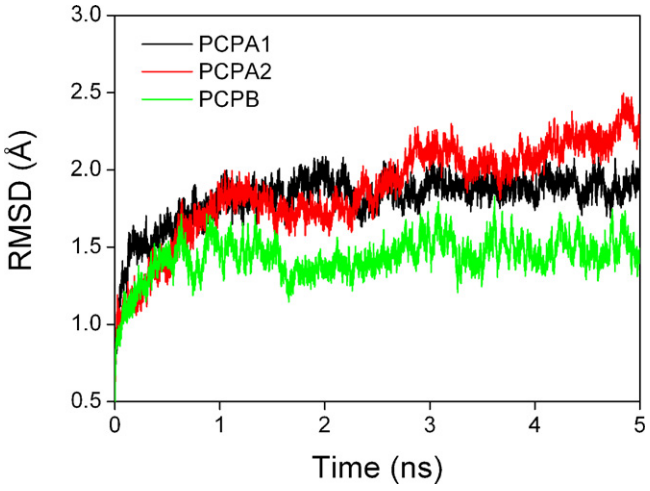

Fig. 2. RMSD profiles of the Cα atoms of three cleaved systems of enzyme–prosegment complexes during 5 ns CMD simulations of PCPA1, PCPA2 and PCPB.

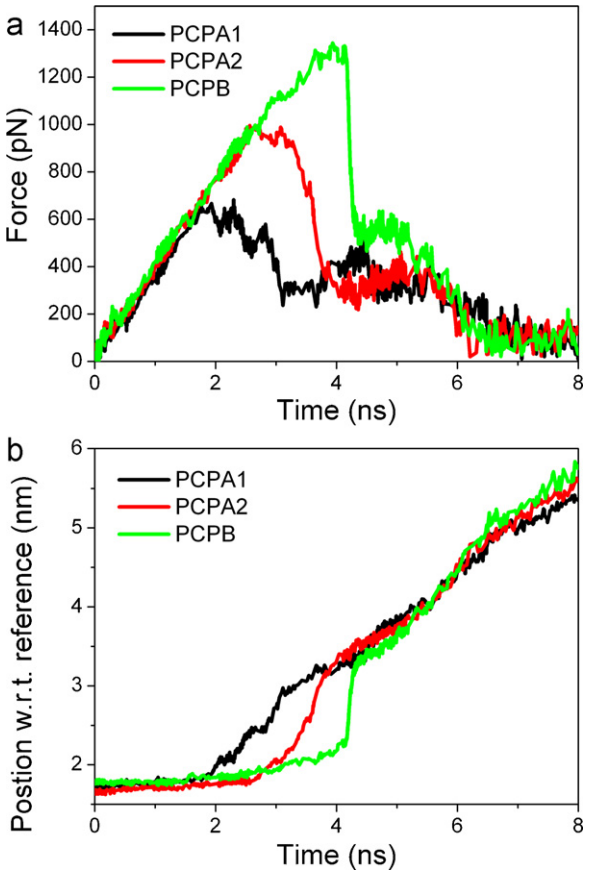

Fig. 3. Force profile (a) and a center-of-mass position (of SMD structure at a particular simulation time) with respect to a reference (of initial SMD structure) (b) obtained from the SMD simulations of prosegment unbinding of PCPA1, PCPA2 and PCPB.

to shed lights on their different rate and mode of activation among the three PCP variants.

In this work, the X-ray structures of zymogens PCPA1, PCPA2 and PCPB were in silico converted into the primary cleavage state of activated zymogens, followed by conventional molecular dynamics (CMD) and steered molecular dynamics (SMD) simulations. Our simulations were performed to mimic a molecular event that associates with the dissociation process of prosegment from the binding site of catalytic domain after the first proteolytic cleavage. This work has considered the possibility that dynamic and long range conformational effects take place after the first proteolytic cleavage in PCPs and our simulations have revealed different releasing mechanisms of the two regions of the prosegment from the enzyme.

2. Computational details

All simulations were performed with GROMACS 3.3.3 [19] using GROMOS96 force field (G43a1) [20] for proteins, the SPC water model, and counter ions including Zn^{2+} ions. Starting zymogen structures used in this study were taken from the X-ray structures of Protein Databank (PDB) (PDB entries 1pca, 1aye and 1nsa for PCPA1, PCPA2, PCPB, respectively). Small molecules such as citric acid and valine in proCPA1 and benzamidine in proCPB were removed while the Zn^{2+} ions and X-ray waters were kept in all systems. The cleaved zymogen model (after the first cleavage) for each system was then examined for the deletion of a peptide bond located on the pro-mature junction where the cleavage takes place [11]: the peptide bonds are covalently formed by residues Arg99p–Ala1 for PCPA1, Arg2–Ser3 for PCPA2 and Arg95p–Thr4 for

Table 1
Comparison of H-bond distances observed at the binding interface of the uncleaved structures from the previous simulations[a] with those of the cleaved structures from the present simulations of PCPA1, PCPA2 and PCPB.

H-bond distances (Å)	Uncleaved	Cleaved (this work)	Δ(distance)
PCPA1			
Key residues[b]			
OD1(Asp36p)···NH1(Arg71)	2.9	3.5	0.6
OD1(Asp53p)···OH(Tyr198)	2.9	3.1	0.2
OE1(Glu89p)···NE(Arg124)	2.8	4.0	1.2
Other residues			
NH2(Arg14p)···O(Thr274)	2.9	4.4	1.5
NH2(Arg39p)···O(Val246)	3.1	6.2	3.1
NH1(Arg47p)···O(Ile244)	2.9	3.2	0.3
OE1(Glu88p)···NH1(Arg277)	2.9	8.2	5.3
O(Ser96p)···ND2(Asn8)	3.1	2.8	–0.3
PCPA2			
Key residues[b]			
OD1(Asp36p)···NH1(Arg71)	2.8	3.3	0.5
ND1(His53p)···OH(Tyr198)	3.0	3.1	0.1
OE1(Glu89p)···NE(Arg124)	2.8	2.9	0.1
Other residues			
OE1(Glu33p)···OG(Ser162)	2.9	5.1	2.2
O(Phe37p)···NH2(Arg71)	3.1	2.8	–0.3
OE1(Glu50p)···NZ(Lys239)	2.9	3.7	0.8
O(Met78p)···NH1(Arg276)	3.0	7.6	4.6
OE2(Glu92p)···NH2(Arg284)	2.9	6.2	3.3
OD1(Asn96p)···ND2(Asn8)	3.0	3.8	0.8
PCPB			
Key residues[b]			
OD2(Asp41p)···NH2(Arg145)	2.9	3.3	0.4
OD1(Asp53p)···OH(Tyr198)	2.8	3.2	0.4
OE1(Gln89p)···NH2(Arg124)	2.8	2.9	0.1
Other residues			
NH2(Arg14p)···O(Lys274)	2.8	3.5	0.7
OD1(Asp36p)···NH1(Arg71)	2.9	3.3	0.4
NZ(Lys39p)···OE1(Glu270)	2.9	9.9	7.0
O(Gln45p)···N(Tyr248)	2.9	4.5	1.6
NZ(Lys47p)···O(Thr246)	3.2	3.9	0.7
NZ(Lys47p)···O(Ser244)	2.8	4.9	2.1
O(Leu78p)···NH1(Arg276)	2.9	3.0	0.1
N(Asp91p)···OE1(Glu283)	3.0	5.3	2.3

Note that salt-bridges are indicated in *italic*.
[a] Distances were taken from MD-average structures from Ref. [18].
[b] Conserved prosegment residues that are predicted to interact strongly with the catalytic domain by simulation [18].

PCPB (see Fig. S1). Note that the nomenclature "p" after each residue means the residue within prosegment, while the residue without this symbol means the residue within the catalytic domain.

The resulting structure was confined in a cubic box neutralized with Na^+ or Cl^- counter ions. The total numbers of atoms including protein, SPC waters and the counter ions are 104,474, 111,515 and 111,571 for PCPA1, PCPA2 and PCPB, respectively. Each system was then energy-minimized with a steepest-descent algorithm for 5000 steps. CMD simulation was performed in NPT ensemble, with temperature and pressure kept constant at 300 K and 1 bar respectively using Berendsen algorithm [21]. Bond lengths were constrained with the LINCS algorithm [22], which allowed an integration step of 2 fs. Lennard–Jones interactions were calculated using a cutoff of 9 Å. At a distance smaller than 9 Å, electrostatic interactions were calculated explicitly, whereas long-range electrostatic interactions were calculated by particle-mesh Ewald summation [23].

Each CMD simulation was first performed for 100 ps, with protein atom positions harmonically constrained (with a force constant of $k = 1000\ \mathrm{kJ\,mol^{-1}\,nm^{-2}}$) while ions and water molecules were free. Then, the simulation was fully relaxed and equilibrated for 5 ns. The coordinates were recorded at every 0.2 ps intervals. After the equilibrated systems were reached, the final structure of this production run served as the starting point for the SMD simulations. It should be noted that multiple snapshots can also be used for obtaining a better statistical analysis; however, only one snapshot used here was good enough for the aim of this study.

The SMD simulations were employed to explore the possible pathway of the prosegment leaving away from the inactive zymogenic form. In every SMD simulations the catalytic domain was fixed in space via a center-of-mass (COM) movement removal of the prosegment. In each system, the COM of the prosegment residues within 3 Å of the reference enzyme was steered away from the mature enzyme (in the x, y, z-direction) with a harmonic potential using a spring force constant of $k = 500\ \mathrm{kJ\,mol^{-1}\,nm^{-2}} = 0.83$ nN/nm. This steering was executed for 8 ns at a constant pulling speed of $v_{\mathrm{pull}} = 0.5$ nm/ns (0.0005 nm/ps). The strong steering potential forces the attached atom to follow it closely. No other atom of the prosegment is restricted in any way, leaving it to respond freely to the forced movement of the attached atom.

3. Results and discussion

3.1. Equilibrium of cleaved zymogens

Before performing SMD simulations to pull the prosegment out of the catalytic domain, three 5 ns CMD simulations of three cleaved zymogens A1, A2 and B were first carried out to make the whole system equilibrated at 300 K and to check a swing of the prosegment during the simulations. Fig. 2 shows the variations of

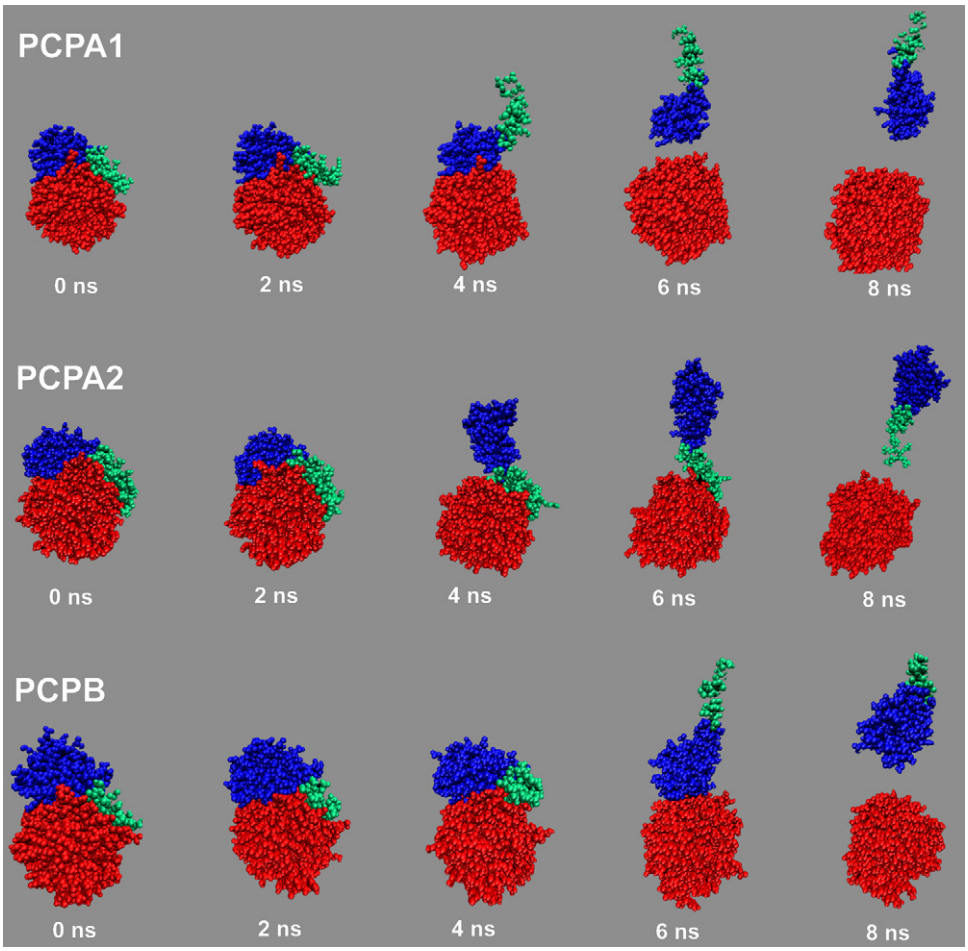

Fig. 4. Snapshots along the trajectory observed during the SMD simulations of the prosegment unbinding for three enzyme–prosegment complex systems of PCPA1, PCPA2 and PCPB. Regions of enzyme domain, globular domain and connecting segment for all systems are colored in red, blue and green, respectively.

root-mean-square deviation (RMSD) values for the Cα atoms of the cleaved zymogens relative to the crystal structures. After 3 ns, the RMSD values for each system fluctuate steadily, implying that the whole system reaches its equilibration state and thus can be used as a starting point for the SMD simulation. As expected, we did not observe any swing of the prosegment towards the enzyme domain throughout the simulation for each system.

3.2. Cleavage effect on hydrogen bond instability

To track a change of hydrogen bond (H-bond) interactions at the binding interfaces of prosegment–enzyme complex upon the cleavage (or cleaved structures), we analyzed the distances of these binding residues based on the present CMD simulations and compared with the H-bond distances taken from average MD structures before cleavage (or uncleaved structures) [18]. The distances for each system are compared and listed in Table 1. It is generally found that most distances from the cleaved structures are lengthened compared to those from the uncleaved ones. The distances for residues located near the cleavage site were largely increased: 2.9–8.2 Å of $OE1^{Glu88p}$—$NH1^{Arg277}$ distance for PCPA1, 3.0–7.6 Å of O^{Met78p}—$NH1^{Arg276}$ distance and 2.9–6.2 Å of $OE2^{Glu92p}$—$NH2^{Arg284}$ distance for PCPA2, and 3.0–5.3 Å of N^{Asp91p}—$OE1^{Glu283}$ distance for PCPB. Interestingly, a minor change of H-bond distances (Δdistance < 1.2 Å, Table 1) was found between residues Asp36p–Arg71, His53p–Tyr198, and Glu89p–Arg124 for PCPA1 and PCPA2 and between Asp41p–Arg145, His53p–Tyr198, and Gln89p–Arg124 for PCPB, implying that these residues may be important for the stability of non-covalent binding of the prosegment–enzyme complex and the releasing pathway of prosegment. Altogether, the first trypic cleavage substantially destabilizes most of the H-bonds at the prosegment–enzyme interface in each zymogen structure.

3.3. Force profile from the SMD simulation

Fig. 3 shows the force profiles and extensions of a COM distance for a particular snapshot relative to a starting point derived from the final CMD simulation. At the beginning of the pulling (Fig. 3a), the forces steadily increase until the first rupture of each system is reached. After the first rupture, each system takes different amount of simulation time before the second rupture takes place: PCPA2 and PCPB spent a shorter period of simulation time (4–8 ns) compared to PCPA1, which required up to 5 ns (from 3 to 8 ns) to complete the unbinding. At the end of the simulations, the pulling forces return to zero, denoting that the prosegment has completely dissociated from the enzyme domain.

Although the force decay patterns of all systems differ significantly at some simulation times, the force profiles were generally found to be similar with two rupture force peaks associated with two disruption stages of the unbinding process. For all systems, the force required for the first dissociation of the complex system was higher than that for the second dissociation. The first and second rupture forces are found to be approximately 680 and 520 pN for PCPA1, 1000 and 460 pN for PCPA2, and 1300 and 600 pN for PCPB. The obtained forces here give us a clear clue for a relatively

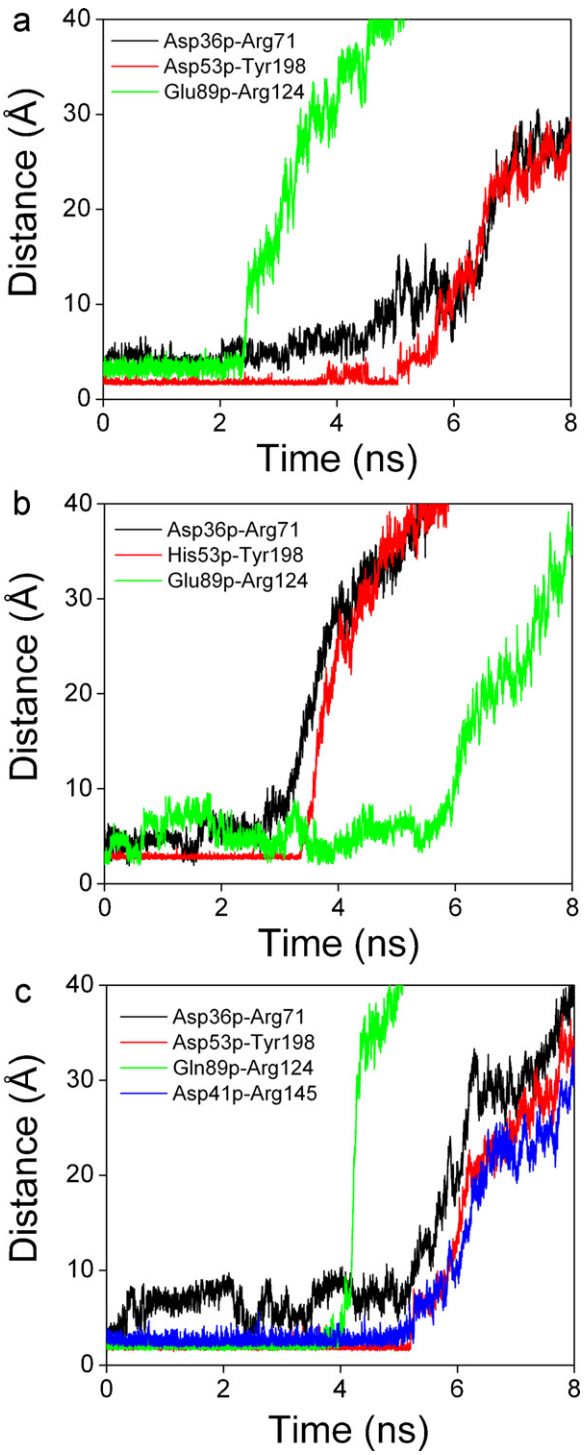

Fig. 5. Distance analysis of the key residues of PCPA1 (a), PCPA2 (b) and PCPB (c).

strong binding between the enzyme and the prosegment of PCPB, compared to the weaker binding at the analogous interfaces of the other two systems of PCPA2 and PCPA1. The high binding affinity of the complex system of PCPB is also in agreement with the strong H-bonds observed from our recent MD simulation [18].

3.4. Conformational change of prosegment upon the pulling process

To obtain more pictures for the prosegment unbinding during the pulling simulations, various snapshots representing the unbinding processes of all systems are provided and illustrated in Fig. 4. During the first 2 ns of the pulling, no conformational change was obvious for all systems evident by a COM distance of <2 Å (see Fig. 3b), except a slight swing at the end of the prosegment in PCPA1 (Fig. 4). A conformational change of each system apparently revealed after 2 ns, as evidenced by a gradual increment in the COM distance shown in Fig. 3b. Remarkably, both PCPA1 and PCPB seem likely to undergo a similar pathway of the prosegment unbinding with the connecting segment releasing first, followed by the globular domain. Meanwhile, PCPA2 conversely undergoes a different conformational change with the globular domain releasing first followed by the connecting segment.

The change in the different conformations of the three prosegment–enzyme complexes during the pulling simulations was found to be associated mainly with the breakdown of some H-bond interactions involving three common prosegment residues of Asp36, Asp53 and Glu89 for proCPA1, Asp36, His53 and Glu89 for proCPA2 and Asp41, Asp53 and Gln89 for proCPB. Such key binding residues were previously found to form tight H-bond interactions during the simulations of zymogen (uncleaved structure) [18]. It was observed that the observed unbinding mechanism in both PCPA1 and PCPB (i.e., the connecting segment releases first) may be due to the weak binding interaction between the connecting segment and the catalytic domain. Specifically, they share a quicker disruption of Glu/Gln89p–Arg124 interaction compared to the other H-bond interactions (i.e., Asp36p–Arg71, Asp53p–Tyr198, Asp41p–Arg145), as shown in Fig. 5a and c, leading to the first release of the connecting segment (Fig. 4). The second rupture occurred as a result of losing two H-bonds formed by residues Asp36p–Arg71 and Asp53p–Tyr198. Note that other residues of Asp36p–Arg71, Asp53p–Tyr198 and Asp41p–Arg145 in PCPB showed breakdown after late 5 ns with the drastic increased distances, indicating the tight binding of these residues associated with the strength of inhibitory globular domain in PCPB.

For PCPA2, the first release of globular domain gives us a clue that the catalytic domain forms a weaker non-covalent binding with the globular domain compared to the binding with the connecting segment. A reason for the weak binding of PCPA2 globular domain can be appreciated from the quick losses of two H-bonds formed between Asp36p–Arg71 and His53p–Tyr198 at ~3 ns (Fig. 5b). Meanwhile, the late breakdown of Glu89–Arg124 interaction in the connecting segment was observed at ~6 ns, which may be due to its intrinsic long alpha-helix that makes the two-domain binding more favorable than the binding from other two PCPs (i.e., PCPA1 and PCPB).

4. Conclusion

Three cleaved zymogens of PCPA1, PCPA2 and PCPB were initially built based on available X-ray structures. Conventional molecular dynamics (CMD) simulations of these models were carried out to obtain the equilibrium states of the whole systems, serving as a starting point for a pulling simulation. We found that the primary cleavage substantially destabilizes most of the H-bonds at the prosegment–enzyme interface in each zymogen structure. By using steered molecular dynamics (SMD) simulations, we were able to pull the prosegment out of the enzyme domain to mimic the activation process of the zymogens A1, A2 and B when the first trypic cleavage presumably occurs and causes full prosegment unbinding. The force profiles from the SMD simulations demonstrated the highest rupture force in PCPB, followed by PCPA2 and PCPA1. Two different unbinding pathways among the three systems were remarkable: PCPA1 and PCPB showed first rupture in the connecting segment followed by the globular domain while PCPA2 conversely showed first rupture in the globular domain and then

the connecting segment. Our simulations have provided insights into the two different unbinding pathways among three cleaved PCP zymogens (types A1, A2 and B) and showed different binding interactions and affinities of the globular domain and connecting segment toward its catalytically binding domain.

Acknowledgements

This work has been supported by the grant from the National Research Council of Thailand. J.J. also thanks the National Electronics and Computer Technology Center, National Science and Technology Development Agency for providing computing resources (http://www.lsr.nectec.or.th).

Appendix A. Supplementary data

Supplementary data associated with this article can be found, in the online version, at http://dx.doi.org/10.1016/j.jmgm.2012.09.002.

References

[1] F.X. Gomis-Ruth, Structure and mechanism of metallocarboxypeptidases, Critical Reviews in Biochemistry and Molecular Biology 43 (2008) 319–345.
[2] J. Vendrell, F.X. Aviles, L.D. Fricker, Metallocarboxypeptidases, Handbook of Metalloproteins 3 (2004) 176–189.
[3] H. Neurath, Evolution of proteolytic enzymes, Science 224 (1984) 350–357.
[4] A.R. Khan, M.N.G. James, Molecular mechanisms for the conversion of zymogens to active proteolytic enzymes, Protein Science 7 (1998) 815–836.
[5] C. Lazure, The peptidase zymogen proregions: nature's way of preventing undesired activation and proteolysis, Current Pharmaceutical Design 8 (2002) 511–531.
[6] F.X. Aviles, J. Vendrell, A. Guasch, M. Coll, R. Huber, Advances in metallo-procarboxypeptidases. Emerging details on the inhibition mechanism and on the activation process, European Journal of Biochemistry 211 (1993) 381–389.
[7] J. Vendrell, C.M. Cuchillo, F.X. Aviles, The tryptic activation pathway of monomeric procarboxypeptidase A, Journal of Biological Chemistry 265 (1990) 6949–6953.
[8] F.J. Burgos, M. Salva, V. Villegas, F. Soriano, E. Mendez, F.X. Aviles, Analysis of the activation process of porcine procarboxypeptidase B and determination of the sequence of its activation segment, Biochemistry 30 (1991) 4082–4089.
[9] D. Reverter, S. Ventura, V. Villegas, J. Vendrell, F.X. Aviles, Overexpression of human procarboxypeptidase A2 in *Pichia pastoris* and detailed characterization of its activation pathway, Journal of Biological Chemistry 273 (1998) 3535–3541.
[10] I. Garcia-Saez, D. Reverter, J. Vendrell, F.X. Aviles, M. Coll, The three-dimensional structure of human procarboxypeptidase A2. Deciphering the basis of the inhibition, activation and intrinsic activity of the zymogen, EMBO Journal 16 (1997) 6906–6913.
[11] J. Vendrell, E. Querol, F.X. Aviles, Metallocarboxypeptidases and their protein inhibitors. Structure, function and biomedical properties, Biochimica et Biophysica Acta, Protein Structure and Molecular Enzymology 1477 (2000) 284–298.
[12] A. Guasch, M. Coll, F.X. Aviles, R. Huber, Three-dimensional structure of porcine pancreatic procarboxypeptidase A. A comparison of the A and B zymogens and their determinants for inhibition and activation, Journal of Molecular Biology 224 (1992) 141–157.
[13] J. Vendrell, A. Guasch, M. Coll, V. Villegas, M. Billeter, G. Wider, et al., Pancreatic procarboxypeptidases: their activation processes related to the structural features of the zymogens and activation segments, Biological Chemistry Hoppe-Seyler 373 (1992) 387–392.
[14] V. Villegas, J. Vendrell, X. Aviles, The activation pathway of procarboxypeptidase B from porcine pancreas: participation of the active enzyme in the proteolytic processing, Protein Science 4 (1995) 1792–1800.
[15] B. Isralewitz, M. Gao, K. Schulten, Steered molecular dynamics and mechanical functions of proteins, Current Opinion in Structural Biology 11 (2001) 224–230.
[16] H. Grubmuller, B. Heymann, P. Tavan, Ligand binding: molecular mechanics calculation of the streptavidin–biotin rupture force, Science 271 (1996) 997–999.
[17] Z. Zuo, C. Gang, H. Zou, P.C. Mok, W. Zhu, K. Chen, et al., Why does beta-secretase zymogen possess catalytic activity? Molecular modeling and molecular dynamics simulation studies, Computational Biology and Chemistry 31 (2007) 186–195.
[18] J. Jitonnom, A.J. Mulholland, Insights into conformational changes of procarboxypeptidase A and B from simulations: a plausible explanation for different intrinsic activity, Theoretical Chemistry Accounts 131 (2012) 1224.
[19] D. Van Der Spoel, E. Lindahl, B. Hess, G. Groenhof, A.E. Mark, H.J. Berendsen, GROMACS: fast, flexible, and free, Journal of Computational Chemistry 26 (2005) 1701–1718.
[20] W.F. van Gunsteren, S.R. Billeter, A.A. Eising, P.H. Hünenberger, P. Krüger, A.E. Mark, W.R.P. Scott, I.G. Tironi, Biomolecular Simulation: The GROMOS96 Manual and User Guide, vdf Hochschulverlag AG, Zürich, 1996.
[21] H.J.C. Berendsen, J.P.M. Postma, W.F. van Gunsteren, A. Di Nola, J.R. Haak, Molecular dynamics with coupling to an external bath, Journal of Chemical Physics 81 (1984) 3684–3690.
[22] B. Hess, H. Bekker, H.J.C. Berendsen, J.G.E.M. Fraaije, LINCS: a linear constraint solver for molecular simulations, Journal of Computational Chemistry 18 (1997) 1463–1472.
[23] T.A. Darden, D.M. York, L.G. Pedersen, Particle mesh Ewald: an N log(N) method for Ewald sums in large systems, Journal of Chemical Physics 98 (1993) 10089–10092.